

## The effects of acidic functional groups and particle size of biochar on Cd adsorption from aqueous solutions

Fardin Sadegh-Zadeh<sup>a</sup>, Abd Wahid Samsuri<sup>b,\*</sup>, Bahi Jalili Seh-Bardan<sup>c</sup>, Mostafa Emadi<sup>d</sup>

<sup>a</sup>Department of Soil Science, Faculty of Agronomy, Sari Agricultural Sciences and Natural Resources University, Sari, Iran, Tel. +989186473262, Fax +981133687568, email: fardin.upm@gmail.com, fardin@sanru.ac.ir

<sup>b</sup>Department of Land Management, Faculty of Agriculture, Universiti Putra Malaysia, 43400 UPM Serdang, Selangor, Malaysia, Tel. +60389474864, Fax +60389408316, email: samsuriaw@upm.edu.my

<sup>c</sup>Department of Soil Science, Faculty of Agronomy, Sari Agricultural Sciences and Natural Resources University, Sari, Iran, Tel. +989166363064, Fax +981133687568, email: b.jalili@sanru.ac.ir

<sup>d</sup>Department of Soil Science, Faculty of Agronomy, Sari Agricultural Sciences and Natural Resources University, Sari, Iran, Tel. +989112532593, Fax +981133687568, email: m.emadi@sanru.ac.ir

Received 17 May 2016; Accepted 5 September 2016

### ABSTRACT

The removal of Cd from the wastewater is necessary because of its harmful health effects. The practice of using biochar as a low-cost adsorbent for heavy metals removal from water bodies is common. However, the effects of total acidic functional groups and particle size class on heavy metals removal by biochar are not studied well. Therefore, this study was undertaken with the objective of determining the effects of total acidic functional groups and particle size class on Cd adsorption from aqueous solution by an empty fruit bunch biochar (EFBB) and a rice husk biochar (RHB). The results showed that there was no significant difference in the carbon content between the EFBB and RHB. However, higher quantity of total acidic functional groups was found in the EFBB compared to the RHB. The total acidic functional groups of EFBB were higher than of the RHB for the same particle size class. In contrast, the surface area of RHB was higher than the EFBB for the same size class. The Langmuir's maximum adsorption capacity ( $Q_{max}$ ) of EFBB was higher than RHB when compared at each particle size class. Significant correlations were observed between  $Q_{max}$  and the total acidic functional groups of both biochars. There were significant correlations between  $Q_{max}$  and the cation exchange capacity (CEC) as well. However, the correlations were non-significant between  $Q_{max}$  and particle size, surface area and pore volume of both biochars. It can be concluded that only the total acidic functional groups and the CEC were influential in determining the adsorption capacities of both EFBB and RHB for Cd adsorption.

*Keywords:* Surface area; Cation exchange capacity; Empty fruit bunch biochar; Rice husk biochar

### 1. Introduction

It is well documented that Cd is toxic to human beings and other living organisms [1]. The sources of Cd contamination in natural water resources includes wastewater discharge from industries such as metal smelting and plating, disposal of Cd-Ni batteries, and the excessive use of phosphate fertilizer. Cadmium toxicity can cause renal

damage, hypertension, proteinuria, kidney stone formation and testicular atrophy [2]. The Cd ions may replace Zn ions in some enzymes thereby affecting the enzyme activity [3]. Therefore, removal of Cd from water bodies is necessary because of its health concerns.

Physical and chemical remediation methods to remove heavy metal pollutants from wastewaters have been extensively studied. Some of these processes are adsorption, coagulation, flotation, biosorption, chemical precipitation, ultra filtration and electrochemical methods. Among these remediation methods, adsorption can be seen as an efficient and economical method to remove

\*Corresponding author.

the heavy metal pollutants at low concentrations. The adsorption of metals by low-cost materials such as biochars from aqueous environments has been reported by numerous studies [4–6]. Chen et al. [7] indicated that biochars derived from hardwood and corn straw were effective as adsorbents for Cu and Zn from an aqueous solution. Liu and Zhang [8] reported that biochars prepared from hydrothermal liquefaction of pinewood and rice husks were able to remove Pb from water. There is a report that revealed biochars produced from rapid pyrolysis of the wood and barks of oaks were able to adsorb Pb and Cd better than a commercial activated carbon per unit surface area [9]. Wang et al. [10] showed that black carbon derived from wheat residues was effective as a low-cost adsorbent for the removal of Cr(VI) from an aqueous solution. The adsorption capacities of sorbents depend on many factors including the type and the amount of surface functional groups [11] and particle size class and specific surface area [12].

Empty fruit bunch is an abundant source of organic waste, which is generated from the oil palm industries. Biochars from empty fruit bunch are manufactured in a large scale. Another abundant source of organic waste is the rice husk, a waste product from rice mills. Biochar derived from rice husks has been produced commercially in Malaysia to avert wastage of large quantities of rice husks [13]. Samsuri et al. [14,15] employed biochars derived from oil palm empty fruit bunches and rice husks for removal of Zn, Cu, Pb and As from aqueous solution and their results showed that these biochars were effective in removing the heavy metals and As from aqueous solutions. However, as far as we know, there is no available data on the effect of acidic surface functional groups and particle size class and specific surface area of commercially produced empty fruit bunch biochar (EFBB) and a rice husk biochar (RHB) on adsorption of Cd from aqueous solutions. Therefore, the objective of this study was to determine the effects of acidic functional groups, particle size class and specific surface area of EFBB and RHB on the adsorption of Cd from aqueous solutions.

## 2.1. Materials and methods

### 2.1. Chemicals

Millipore® water was used to prepare all solutions throughout this study. Cadmium chloride was purchased from Sigma-Aldrich. Stock solution ( $1000 \text{ mg L}^{-1}$ ) of Cd was prepared from its analytical grade compounds in Millipore® water. The pH of stock solution was adjusted to 6 using concentrated  $\text{HNO}_3$ . All other chemicals used were analytical reagent grade purchased from Sigma-Aldrich (Seelze, Germany). Hydrochloric acid (1.0 M HCl) and sodium hydroxide (1.0 M NaOH) were used to adjust the pH to the desired values throughout the batch experiments.

### 2.2. Biochars characterization

Both the EFBB and the RHB were purchased locally. The biochars were purchased from Nasmeh Technology Sdn. Bhd. in Selangor, Malaysia. According the company;

electrically heated rotating pyrolysis reactor was used to produce biochars. The sample was heated up to  $300^\circ\text{C}$  for 3 h at heating rate  $3^\circ\text{C}/\text{min}$  with 0.5 RPM. The biochar moisture content was measured by oven drying 5 g of a sample at  $105^\circ\text{C}$  for 24 h, and the moisture content was calculated by the difference between the weights of fresh and oven-dried samples. The pH was measured in a 0.5:100 (w/v) biochar: water suspension. The concentrations of K, Ca, Mg, P, Mn, Fe, Cu, and Na were determined using the ASTM D5142 method [16]. Ash contents were determined by combusting the EFBB and RHB at  $700^\circ\text{C}$  for 12 h in open crucibles. The carbon, hydrogen, nitrogen, sulfur, and oxygen components of biochar samples were determined using a CHNSO elemental analyzer (Perkin Elmer 2400 Series II CHNSO Elemental Analyzer, Germany).

### 2.3. Scanning electron microanalysis

The surface morphology of the EFBB and RHB before and after adsorption of Cd was examined using a scanning electron microscope at 15 keV, equipped with energy dispersive X-ray spectroscopy (JEOL, JSM-6400V, Japan). The scanning electron microscopy (SEM) analysis was carried out before and after the adsorption of Cd. The biochar samples used for this study were obtained from the batch equilibrium adsorption experiment in which 0.2 g of biochar was shaken in 40 mL of solution containing  $100 \text{ mg L}^{-1}$  of Cd.

### 2.4. The effects of solution pH on Cd precipitation

To distinguish between the adsorption and the precipitation process of Cd in solutions, the precipitation of Cd was examined in solutions with varying pHs. Briefly, the solutions were non-buffered and their pHs were adjusted to pH between 2 to 9 using either 0.1 M NaOH or 0.1 M HCl. The Cd was added to solutions to obtain solutions containing  $100 \text{ mg L}^{-1}$  of Cd and then shaken for 24 h, after which the solutions were centrifuged at 1000 rpm for 10 min. The supernatant solutions were then analyzed for their Cd concentrations using Perkin Elmer Optima 8300, ICP-OES (USA).

### 2.5. The effects of solution pH on Cd adsorption

The adsorption of Cd was studied at different pHs. The pH was adjusted to pH between 2 to 7, using either 0.1 M NaOH or 0.1 M HCl. The adsorption procedure was similar to the procedure described in the batch equilibrium adsorption, except that in this study only one concentration of Cd was used,  $100 \text{ mg L}^{-1}$ . The concentration of the remaining Cd in the solution was measured after 24 h of equilibration.

### 2.6. Classification of biochar particle sizes

The biochars were separated into different sizes by wet sieving using 2.83, 2, 1, 0.25, 0.053 mm mesh sizes sieves and also a  $0.45 \mu\text{m}$  pore size membrane filter. Each biochar sample was immersed in deionized water for 2 h. The sample was then wet-sieved using a motor-driven holder

lowering the sieves in a container of deionized water. The stroke length was 1.3 cm and the sieving frequency was 35 cycles  $\text{min}^{-1}$  for 10 min. Each fraction was collected from the sieve and dried at 105°C for 24 h. The solution containing fine particles of biochar which passed through the 53  $\mu\text{m}$  sieve was collected and then it was passed through a 0.45  $\mu\text{m}$  pore size membrane filter. The biochar particles which remained on the membrane filter were dried at 105°C for 24 h. Hereafter, the EFBB which remained on the sieves with 2.83, 2, 1, 0.25, 0.053 mm mesh sizes and 0.000045 mm pore size membrane filter were denoted as EFBB2.83, EFBB2, EFBB1, EFBB0.25 and EFBB0.053 and EFBB0.000045 respectively. The RHB which remain on the sieves with 2.83, 2, 1, 0.25, 0.053 mm mesh sizes and 0.000045 mm pore size membrane filter were denoted as RHB2.83, RHB2, RHB1, RHB0.25, RHB0.053 and RHB0.000045, respectively.

### 2.7. Measurements of biochar cation exchange capacity (CEC)

Briefly, 0.2 g of biochar was put into a centrifuge tube and 34 mL of 1.0 N NaOAc solution was added. The suspension was shaken on a mechanical shaker for 5 min, and then centrifuged for 5 min at 10,000 rpm. The supernatant was decanted. Again, 33 mL of 1.0 N NaOAc solution was added to centrifuge tube and the same process was repeated. Finally, 33 mL of 99% isopropyl alcohol was added to centrifuge tube, the tube was shaken, centrifuged and the supernatant was decanted. This procedure was further repeated for 2 more times. For substituting the adsorbed Na on biochar particles, 34 mL of  $\text{NH}_4\text{OAc}$  solution was added to the centrifuge tube. It was shaken for 5 min and then centrifuged for 5 min at 10,000 rpm. Then, the supernatant was decanted into a 100-mL volumetric flask. This procedure was replicated for 2 times and the Na concentration in the solution was determined by flame photometer (Model PFP7/C, England).

### 2.8. Determination of biochar surface area and acidic functional groups

The surface area of the biochar was measured with  $\text{N}_2$  adsorption at 77.3 K, using a Quantachrome version 2.01 (Quantachrome AS1Win™, Germany) surface area analyzer. The biochar sample was degassed at 100°C for 9 h prior to  $\text{N}_2$  adsorption. The multipoint Brunauer-Emmett-Teller (BET) method was employed to calculate the total surface area. The pore volumes, pore radii and internal surface areas (pore surface areas) were obtained from the desorption isotherms, using the Barrett-Joyner-Halenda (BJH) method. Four data points with relative pressures of 0.05–0.3 were used to construct the monolayer adsorption capacity. The total pore volume was estimated from a single  $\text{N}_2$  adsorption point at a relative pressure of approximately 0.97.

The contents of acidic surface functional groups were measured using the base titration methods [17]. Briefly, an aliquot (0.2 g) of each biochar was soaked with 20 mL of different base solutions (0.1 M NaOH, 0.1 M  $\text{Na}_2\text{CO}_3$ , and 0.05 M  $\text{NaHCO}_3$ ) and shaken for 24 h and shaken at a room temperature. The solutions were passed through a 0.45  $\mu\text{m}$  pore size membrane filter. Precisely a 10 mL solution was pipetted into a 100-mL conic glass flask, followed

by the addition of 15 mL 0.1 M HCl and back titrated with freshly standardized 0.1 M NaOH to endpoints using phenolphthalein as the indicator. The NaOH-titrable and  $\text{NaHCO}_3$ -titrable acidities were treated as the total acidic surface functional groups and carboxyl groups, respectively. The difference between NaOH-titrable and  $\text{Na}_2\text{CO}_3$ -titrable acidity was attributed to phenol groups and the difference between  $\text{Na}_2\text{CO}_3$ -titrable and  $\text{NaHCO}_3$ -titrable acidity was attributed to lactone groups.

### 2.9. Batch equilibrium adsorption

The experiment was carried out at  $25 \pm 1^\circ\text{C}$ . About 0.2 g of each biochar was transferred to centrifuge tubes containing 40 mL of 3 to 300  $\text{mg L}^{-1}$  Cd solutions at pH 6. The optimum equilibrium time and sorbent concentration for the batch equilibrium method were priorly determined to be 24 h and 5  $\text{g L}^{-1}$ , respectively. The centrifuge tubes were shaken on a rotary shaker at 40 rpm for 24 h and then centrifuged at 7,000 rpm for 10 min. The supernatants were passed through Watman No. 42 filter paper and the filtrates were analyzed for their Cd concentrations using Perkin Elmer Optima 8300, ICP-OES. All experiments were conducted in triplicate. To evaluate and compare the adsorption capacities of the biochars and biochar particles size distributions for Cd, the Langmuir adsorption model was used to fit the sorption data. The equation of Langmuir's adsorption model is as follow:

$$\text{Langmuir, } q_e = Q_{\max} bC_e / (1 + bC_e)$$

where  $q_e$  is the amount of the metal adsorbed per unit weight of biochar ( $\text{mg g}^{-1}$ );  $C_e$  is the equilibrium concentration of metal in solution ( $\text{mg L}^{-1}$ );  $Q_{\max}$  is the maximum adsorption capacity ( $\text{mg g}^{-1}$ ) and  $b$  is the constant related to the affinity. The values of  $Q_{\max}$  and  $b$  were determined from the linearized form of the Langmuir equation.

## 3. Results and discussion

### 3.1. Physicochemical properties of the EFBB and RHB

The selected physicochemical properties of the EFBB and RHB are shown in Table 1. There was no significant difference between the carbon content of the EFBB and RHB. However, the concentrations of O, H, S, N and K in the EFBB were much higher than in the RHB. In contrast, the amount of Si was higher in the RHB. The molar ratios of hydrogen to carbon (H/C) for the EFBB and RHB were 0.08 and 0.05, respectively. These amounts are much lower than the reported value obtained from an activated carbon, which was 0.256 [18]. The degree of carbonization can be estimated from the H/C molar ratio [19]. The low H/C molar ratios for both biochars suggest that they contained low amounts of the original plant organic residues, such as cellulose, but high carbonization [20]. The molar ratio of oxygen to carbon (O/C) of biochars has been used as an indicator for surface hydrophilicity because it is indicative of the polar-group content derived from carbohydrates [20]. The O/C molar ratio for the EFBB (0.67) was higher than for the RHB (0.37). The O/C molar ratios of both bio-

Table 1  
The selected physiochemical characteristics of the EFBB and RHB

Parameters	EFBB	RHB
Moisture content (%)	2.00	3.70
Ash content (%)	13.9	27.2
pH	9.4	8.50
C (%)	48.0	45.0
O (%)	30.0	17.0
H (%)	3.80	2.30
S (%)	0.50	0.20
N (%)	1.30	0.17
K (%)	5.40	0.09
Si (%)	0.80	11.00
H/C molar ratio	0.08	0.05
O/C molar ratio	0.61	0.37
(O + N)/C molar ratio	0.64	0.38
Al (mg kg <sup>-1</sup> )	350	189
Ca (mg kg <sup>-1</sup> )	792.00	671.00
Mg (mg kg <sup>-1</sup> )	414.00	357.00
Na (mg kg <sup>-1</sup> )	63.00	75.00
P (mg kg <sup>-1</sup> )	587.00	638.00
Fe (mg kg <sup>-1</sup> )	23.00	45.00
Mn (mg kg <sup>-1</sup> )	8.00	13.00

chars were high in comparison to the values reported by Chen et al. [18], which suggest the hydrophilic nature of the EFBB and RHB. The EFBB had a higher polarity index

[(O+N)/C] than the RHB, which indicates a higher concentration of surface polar functional groups in the EFBB [18]. The RHB had higher total surface, pore surface area and pore volume than the EFBB. There was no significant difference between the Na, P, Ca and Mg contents of the EFBB and RHB but the concentrations of Al and K in the EFBB were higher than the RHB. The contents of Mg and Ca in the both biochars were in the similar range of those reported in the literature [21].

Surface area (SA), pore volume (PV), cation exchange capacity (CEC) and acidic functional groups of each EFBB and RHB particle size class.

The SA, PV, CEC, acidic functional groups (carboxylic, phenolic and lactone) of each EFBB and RHB particle size class are shown in Table 2. The SA of EFBB increased significantly with decreasing particles size. The EFBB2.83 had the lowest surface area (0.5 m<sup>2</sup> g<sup>-1</sup>) and EFBB0.000045 had the highest SA (2.5 m<sup>2</sup> g<sup>-1</sup>) among the EFBB particles size class. The PV of EFBB had the same trend as the SA. The EFBB2.83 had the lowest PV (0.008 cm<sup>3</sup> g<sup>-1</sup>) while EFBB0.000045 had the highest PV (0.019 cm<sup>3</sup> g<sup>-1</sup>). However, there was no obvious trend in total acidic functional groups of EFBB with particle size class. The EFBB0.053 had the highest total acidic functional groups (141 cmolH<sup>+</sup> kg<sup>-1</sup>) while the lowest total acidic functional groups (117 cmolH<sup>+</sup> kg<sup>-1</sup>) was observed in the EFBB2.83. The CEC of EFBB was highest for EFBB0.053 (73 cmol<sub>c</sub> kg<sup>-1</sup>) while EFBB2.83 had the lowest CEC (60 cmol<sub>c</sub> kg<sup>-1</sup>).

The SA of RHB increased significantly with decreasing particles size. Among the RHB particle size classes, the RHB2.83 had the lowest surface area (3 m<sup>2</sup> g<sup>-1</sup>) while RHB0.000045 had the highest SA (17 m<sup>2</sup> g<sup>-1</sup>). Similar trend was observed for the SA. The RHB2.83 had the lowest PV

Table 2  
The  $Q_{max}$ , surface area (SA), pore volume (PV), cation exchange capacity (CEC), acidic functional groups (carboxylic, phenolic and lactone) of classified particle sizes of EFBB and RHB

EFBB		$Q_{max}$ (mg g <sup>-1</sup> )	SA (m <sup>2</sup> g)	PV (cm <sup>3</sup> g <sup>-1</sup> )	CEC (cmol <sub>c</sub> kg <sup>-1</sup> )	Carboxylic (cmolH <sup>+</sup> kg <sup>-1</sup> )	Phenolic (cmolH <sup>+</sup> kg <sup>-1</sup> )	Lactone (cmolH <sup>+</sup> kg <sup>-1</sup> )	Total (cmolH <sup>+</sup> kg <sup>-1</sup> )
Particle size class (mm)	Symbols								
>2.83	EFBB2.83	76	0.5	0.008	59	60	25	22	117
2–2.83	EFBB2	80	0.8	0.009	63	58	37	28	123
1–2	EFBB1	86	1	0.011	68	65	40	29	132
0.25–1	EFBB0.25	83	1.3	0.014	65	61	39	29	125
0.053–0.25	EFBB0.053	101	1.7	0.016	71	73	40	28	141
0.000045–0.053	EFBB0.000045	82	2.5	0.019	66	66	35	26	127
RHB		$Q_{max}$ (mg g <sup>-1</sup> )	SA (m <sup>2</sup> g)	PV (cm <sup>3</sup> g <sup>-1</sup> )	CEC (cmol <sub>c</sub> kg <sup>-1</sup> )	Carboxylic (cmolH <sup>+</sup> kg <sup>-1</sup> )	Phenolic (cmolH <sup>+</sup> kg <sup>-1</sup> )	Lactone (cmolH <sup>+</sup> kg <sup>-1</sup> )	Total (cmolH <sup>+</sup> kg <sup>-1</sup> )
Particle size class (mm)	Symbols								
>2.83	RHB2.83	34	3	0.018	21	17	12	11	39
2–2.83	RHB2	35	5	0.019	22	17	14	9	40
1–2	RHBB1	39	8	0.020	23	17	12	13	42
0.25–1	RHB0.25	45	10	0.022	25	22	14	11	45
0.053–0.25	RHB0.053	32	13	0.023	20	15	13	9	37
0.000045–0.053	RHB0.000045	30	17	0.026	18	13	10	11	34

( $0.018 \text{ cm}^3 \text{ g}^{-1}$ ) and EFBB0.000045 had highest the PV ( $0.026 \text{ cm}^3 \text{ g}^{-1}$ ). However, there was no specific trend in total acidic functional groups of RHB with particle size class. The RHB0.025 had the highest total acidic functional groups ( $45 \text{ cmolH}^+ \text{ kg}^{-1}$ ) and RHB0.000045 had the lowest total acidic functional groups ( $34 \text{ cmolH}^+ \text{ kg}^{-1}$ ). Similarly, there was no specific trend for the CEC of RHB with particle size class. The RHB0.025 had highest the CEC ( $25 \text{ cmol}_c \text{ kg}^{-1}$ ) and RHB0.000045 had the lowest total acidic functional groups ( $18 \text{ cmol}_c \text{ kg}^{-1}$ ).

In general, for a similar particle size class the SA and PV of RHB are higher than the SA and PV of EFBB. The SA and PV of RHB0.000045 for example, were  $17 \text{ (m}^2 \text{ g}^{-1})$  and  $0.026 \text{ (cm}^3 \text{ g}^{-1})$ , respectively. The SA and PV of EFBB0.000045 were  $2.5 \text{ (m}^2 \text{ g}^{-1})$  and  $0.019 \text{ (cm}^3 \text{ g}^{-1})$ , respectively. However, the CEC and total acidic functional groups of classified of RHB are lower than the EFBB for the same particle size class. For example, the CEC and total acidic functional groups of RHB0.000045 were  $18 \text{ (cmol}_c \text{ kg}^{-1})$  and  $34 \text{ (cmolH}^+ \text{ kg}^{-1})$ , respectively, while the CEC and total acidic functional groups of EFBB0.000045 were  $88 \text{ (cmol}_c \text{ kg}^{-1})$  and  $127 \text{ (cmolH}^+ \text{ kg}^{-1})$ , respectively.

### 3.2. The effects of solution pH on Cd precipitation

Fig. 1 shows the concentrations of Cd remained in solutions at different pHs from the initial  $100 \text{ mg L}^{-1}$  concentration after being equilibrated for 24 h. The Cd concentration was less than  $100 \text{ mg L}^{-1}$  at pHs above 6 suggesting that some of the Cd was precipitated at these pHs. The amount of Cd precipitated at the pH of 7, 8 and 9 were 2, 8 and 13%, respectively. The main mechanism for precipitation of heavy metals in solution is complexation with hydroxyl ions [22]. The pHs of these solutions dropped after Cd dropped which suggest the formation of  $\text{Cd(OH)}_2$  complex.

### 3.3. The effect of solutions pH on Cd adsorption

The amounts of Cd adsorbed by the EFBB and RHB at different pHs are presented in Fig. 2. The amount of Cd adsorbed from the solution increased with increasing pH

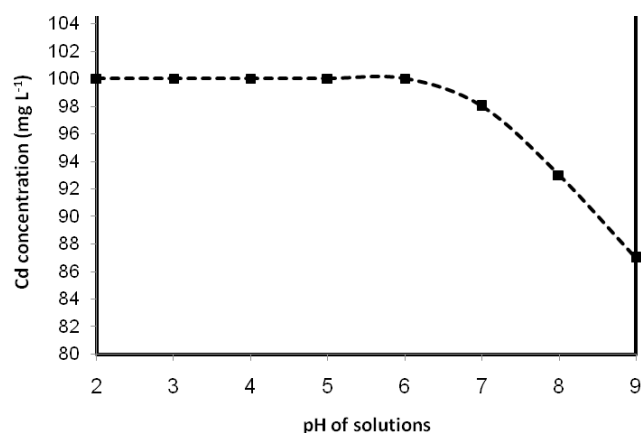


Fig. 1. The concentrations of Cd remaining in the solutions at different pHs from the initial concentration of  $100 \text{ mg L}^{-1}$ .

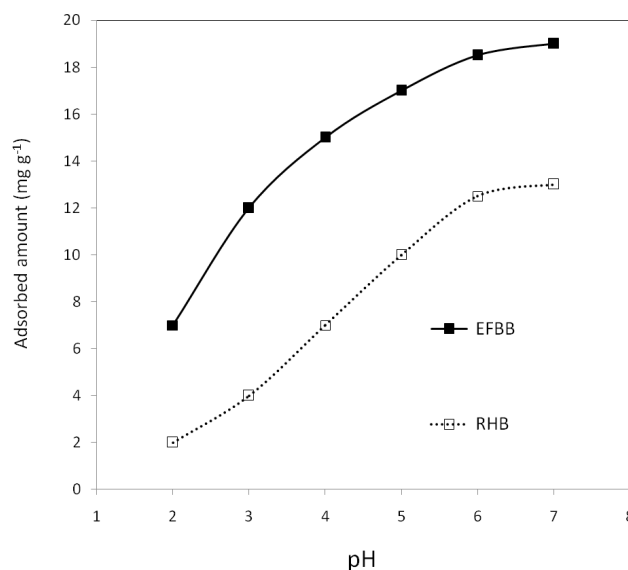


Fig. 2. The amounts of Cd adsorbed by the EFBB and RHB at different pHs.

for both sorbents and the maximum adsorption occurred at pH 7. However, the batch equilibrium isotherm of Cd adsorption by each biochar particles size class was conducted at pH 6 since Cd precipitated at pH 7 (Fig. 1).

### 3.4. Scanning electron microanalysis

The SEM micrographs for the EFBB and RHB before and after adsorption of Cd are shown in Fig. 3. The surface morphology of the EFBB was smooth prior to adsorption of Cd (Fig. 3a) but became coarser after the adsorption of Cd (Fig. 3c). The energy dispersive spectroscopy (EDS) spectra of the EFBB before and after Cd adsorption are shown in Fig. 3b and 3d, respectively. The data indicated the presence of C, O, Mg, K, Ca and P on the surface of the EFBB before Cd adsorption, but Cd was not detected (Fig. 3a). After adsorption, Cd was present on the surface (Fig. 3d), confirming that adsorption had occurred. The SEM micrograph of RHB before Cd adsorption is shown in Fig. 3e. There was a change in surface of RHB after adsorption of Cd (Fig. 3g). The adsorption of Cd by RHB is confirmed by the EDS spectra (Fig. 3h).

### 3.5. Batch equilibrium adsorption

The isotherm adsorption data were fitted to the Langmuir's adsorption model. The Langmuir's adsorption model fits the adsorption data well, as indicated by the high  $R^2$  values. The maximum adsorption capacity ( $Q_{max}$ ) of each EFBB and RHB particle size classes are shown in Table 2. The highest and lowest  $Q_{max}$  among the particle size classes of EFBB were EFBB0.053 and EFBB2.83, respectively. The  $Q_{max}$  of the different EFBB particle size classes were the following descending order: EFBB0.053 > EFBB1 > EFBB0.025 > EFBB0.000045 > EFBB2 > EFBB2.83 (Table 2).

The highest and the lowest  $Q_{max}$  values among the different particle size classes of RHB were RHB0.25 and

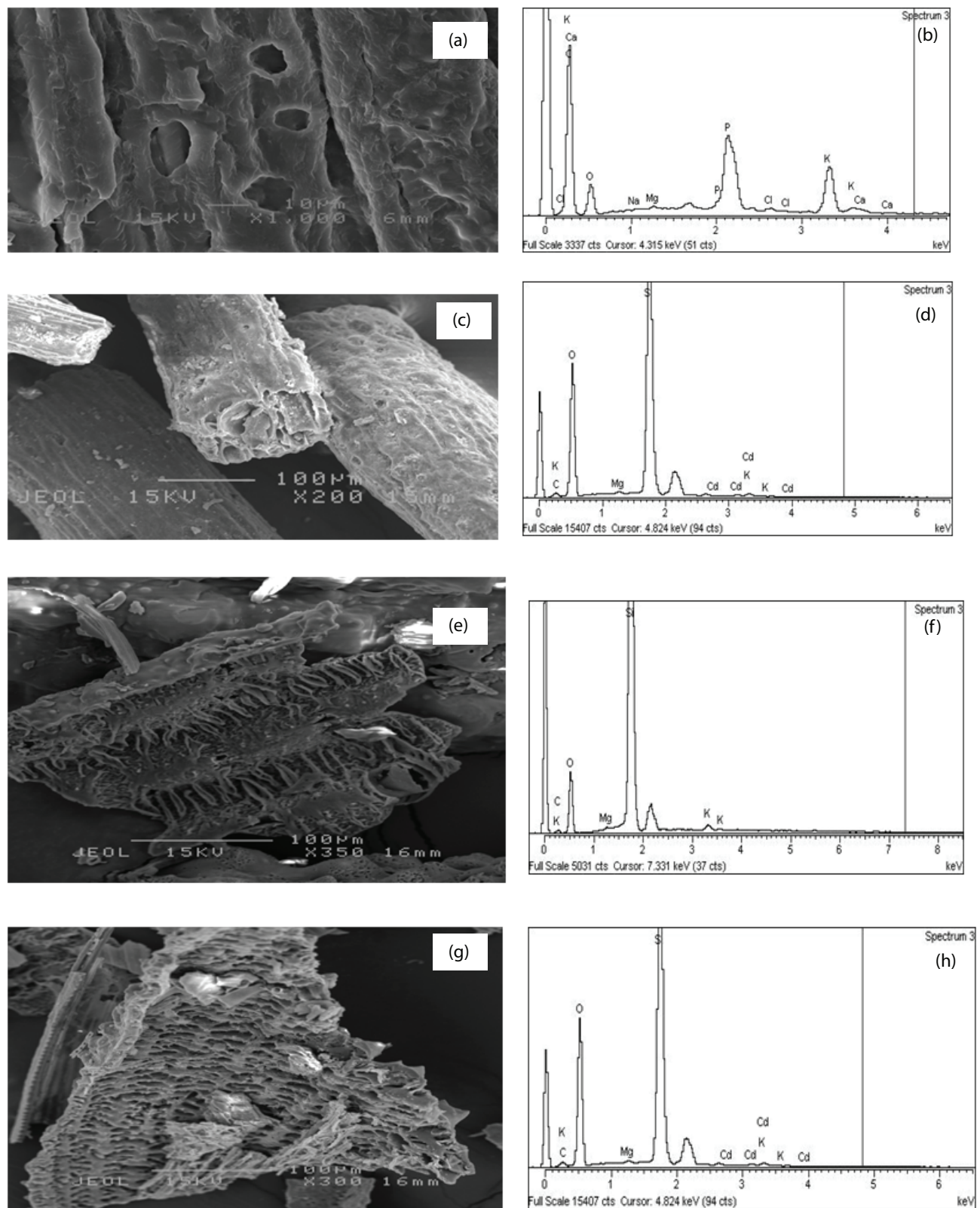


Fig. 3. The SEM micrographs for the EFBB and RHB before and after adsorption of Cd: (a) surface of the EFBB before Cd adsorption; (b) EDS spectrum of the EFBB before adsorption of Cd; (c) surface of the EFBB after Cd adsorption; (d) EDS spectrum of the EFBB after adsorption of Cd; (e) surface of the RHB before Cd adsorption; (f) EDS spectrum of the RHB before adsorption of Cd; (g) surface of the RHB after Cd adsorption; (h) EDS spectrum of the RHB after adsorption of Cd. The EDX spectra are taken from the area indicated by the squares in the micrographs.

RHB0.000045, respectively. The  $Q_{max}$  values for each RHB particle size class were the following in descending order: RHB0.25 > RHB1 > RHB2 > RHB2.83 > RHB0.000045 (Table 2). The  $Q_{max}$  values for EFBB were much higher than the RHB for the same particle size classes. The lowest  $Q_{max}$  among the different particle sizes classes of EFBB ( $76 \text{ mg g}^{-1}$ ) was even higher than the highest  $Q_{max}$  among the RHB particle size classes ( $45 \text{ mg g}^{-1}$ ). The  $Q_{max}$  of EFBB observed in this study was much higher than the  $Q_{max}$  values reported by other researchers for the same particle size classes (Table 3). The  $Q_{max}$  values obtained for RHB (Table 2) were either equal or higher than some of the reported results for similar particle size classes (Table 3). Since the EFBB had a higher adsorption capacity, it was found to be the most effective adsorbent for removing Cd from aqueous solutions in comparison to other adsorbents (Table 3). Therefore, it can be concluded that both EFBB and RHB were effective adsorbents for Cd removal from the aqueous solutions.

### 3.6. Correlation between $Q_{max}$ and the properties of biochars

Fig. 4 shows the correlation between  $Q_{max}$  and EFBB characteristics. There was a significant correlation ( $P < 0.05$ ) between the  $Q_{max}$  of classified particles size of EFBB and their total acidic functional groups (Fig. 4a). The  $Q_{max}$  was increased as the amount of total acidic functional groups enhanced. This result indicated that the acidic functional groups had influence on Cd adsorption. In addition, there was a significant correlation ( $P < 0.05$ ) between the  $Q_{max}$  of EFBB from different size classes classified particles size of EFBB and their CECs (Fig. 4b). The  $Q_{max}$  was increased as the CEC of classified EFBB particles size enhanced. Therefore, it can be concluded that CEC properties of biochar had important role on Cd adsorption.

The correlation between the  $Q_{max}$  and EFBB particles size is shown in Fig. 4c. The correlation between the  $Q_{max}$  and EFBB particles size was statistically significant but it was low ( $r = 0.402$ ). This revealed that effectiveness of EFBB particles size on Cd adsorption was less than total

functional acidic groups and CEC of EFBB. The correlation between the  $Q_{max}$  and EFBB surface area and EFBB pore volume are shown in Fig. 4d and 4e, respectively. The correlation between  $Q_{max}$  and EFBB surface area and EFBB pore volume were non-significant. Hence, the SA and PV of EFBB had no effect on Cd adsorption. Therefore, it can be concluded from the results that the EFBB total acidic functional groups and CEC had important roles on Cd adsorption while the EFBB particle size, surface area and pore volume had insignificant roles on Cd adsorption.

Fig. 5 shows the correlation between  $Q_{max}$  and RHB characteristics. There was a significant correlation ( $P < 0.05$ ) between the  $Q_{max}$  of RHB and the total acidic functional groups and CEC of RHB (Fig. 5a and 5b). The correlation between the  $Q_{max}$  and RHB particles size, SA and PV are shown in Fig. 5c, 5d and 5e, respectively. The correlation between the  $Q_{max}$  and particles size, SA and PV of RHB were non-significant. The  $Q_{max}$  was increased as the amount of total acidic functional groups and CEC enhanced. This result indicated that the acidic functional groups and CEC had influence on Cd adsorption. Therefore, it can be concluded that only the total acidic functional groups and CEC of RHB had considerable effect on Cd adsorption by RHB. This result was similar to the consequence which obtained for correlation of  $Q_{max}$  and EFBB acidic functional groups and CEC of EFBB. It is obvious that the acid functional groups and CEC were the important properties that determined Cd adsorption by both the EFBB and RHB.

These results are in agreement with the results of Yenisooy-Karakas et al. [11] who showed the type and concentration of surface functional groups has important impact on the adsorption capacity and the removal mechanism of the adsorbates by biochars. In addition, the results are also consistent with the results of other researches [19,31,32] that acidic functional groups were effective in removal of heavy metals from aqueous solutions. However, our results is in contrast with the results of Chen et al. [7] that showed biochar produced from hard wood pyrolysed at  $450^\circ\text{C}$  contained a larger amount of oxygen-containing functional groups, and a higher O/C ratio than biochar produced from corn straw at  $600^\circ\text{C}$  but the former had a lower adsorption capacity for heavy metals than the corn straw biochar.

The correlation between the  $Q_{max}$  and RHB particles size, SA and PV are shown in Fig. 5c, 5d and 5e, respectively. The correlation between the  $Q_{max}$  and particles size, SA and PV of RHB were non-significant. Hence, the particles size, SA and PV of RHB had no effect on Cd adsorption. This result is in contrast with result of Chen et al. [7] that suggested that surface area of biochar may therefore be more important than the presence of specific functional groups when it comes to metal binding. However, Chen et al. [7] experiments were done using two different biochars which had different pHs; one had a pH of 5 and the other had a pH of 10. The conclusion was according to surface area and functional groups of biochars and they did not determine biochar pH effects on removal (adsorption and precipitation) of heavy metals, while one of that biochar had a pH5 and the other had pH 10. Since, our previous study [15] revealed that the pH of both biochar and the solution showed that the biochars's

Table 3  
Maximum Cd adsorption capacities of various adsorbents

Adsorbent	$Q_{max}$ ( $\text{mg g}^{-1}$ )	Reference
Chitin	16	Benguella and Benaissa, [23]
Granular activated carbon	10	Moreno-Castilla et al. [24]
Bacteria	19	Huang et al. [25]
Rice husk	21	Kumar et al. [26]
Ficus religiosa leaf powder	27	Rao et al. [27]
Modified kaolinite clay	43	Unuabonah et al. [28]
Nanostructured goethite	29	Mohapatra et al. [29]
Dairy manure-derived biochar	32	Xu et al. [30]
RHB (mean of all size classes)	36	Present study
EFBB (mean of all size classes)	85	Present study

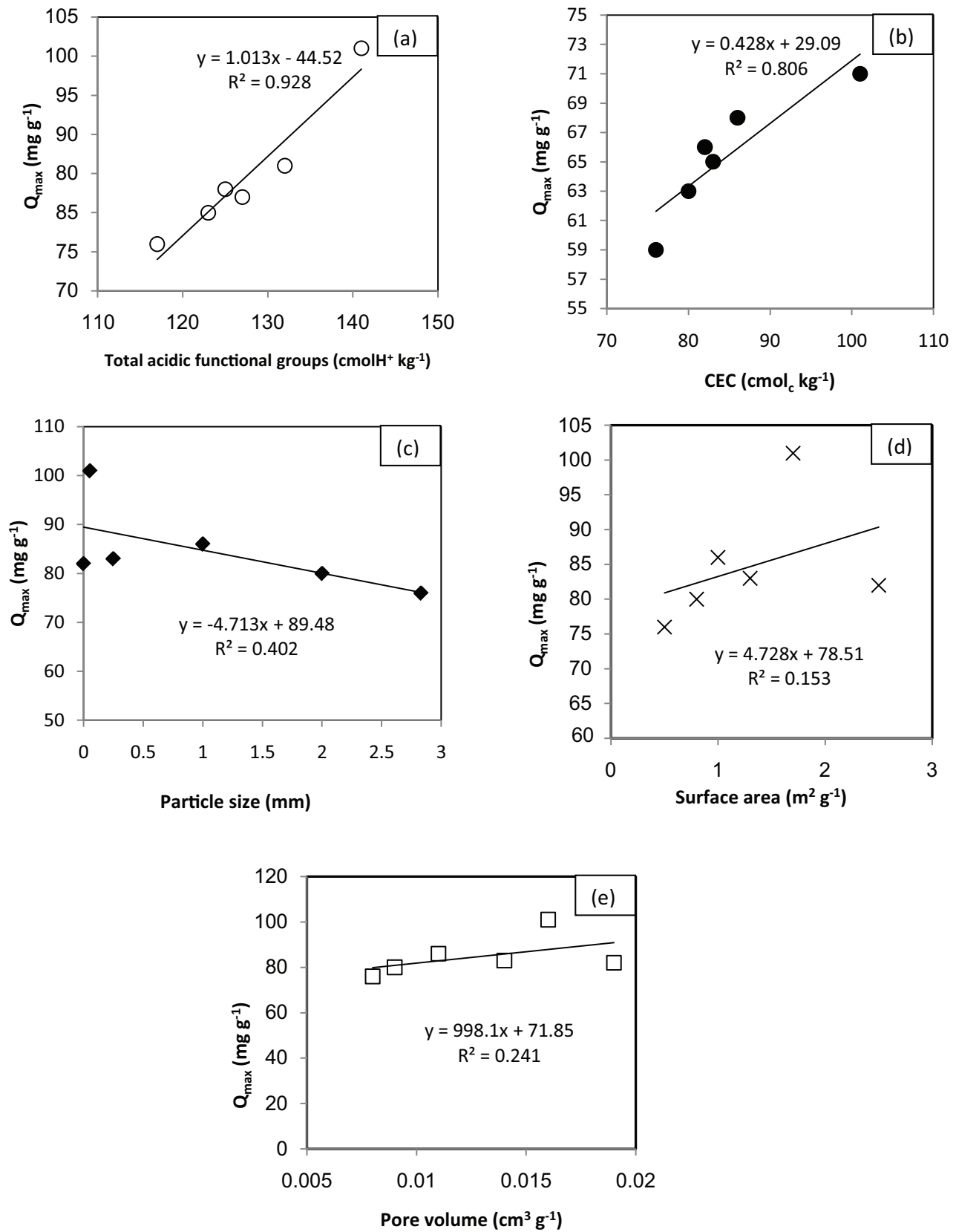


Fig. 4. Correlation between maximum adsorption capacity ( $Q_{max}$ ) of EFBB and its characteristics: (a) total acidic functional groups; (b) cation exchange capacity (CEC); (c) particles size; (d) surface area (SA); (e) pore volume (PV).



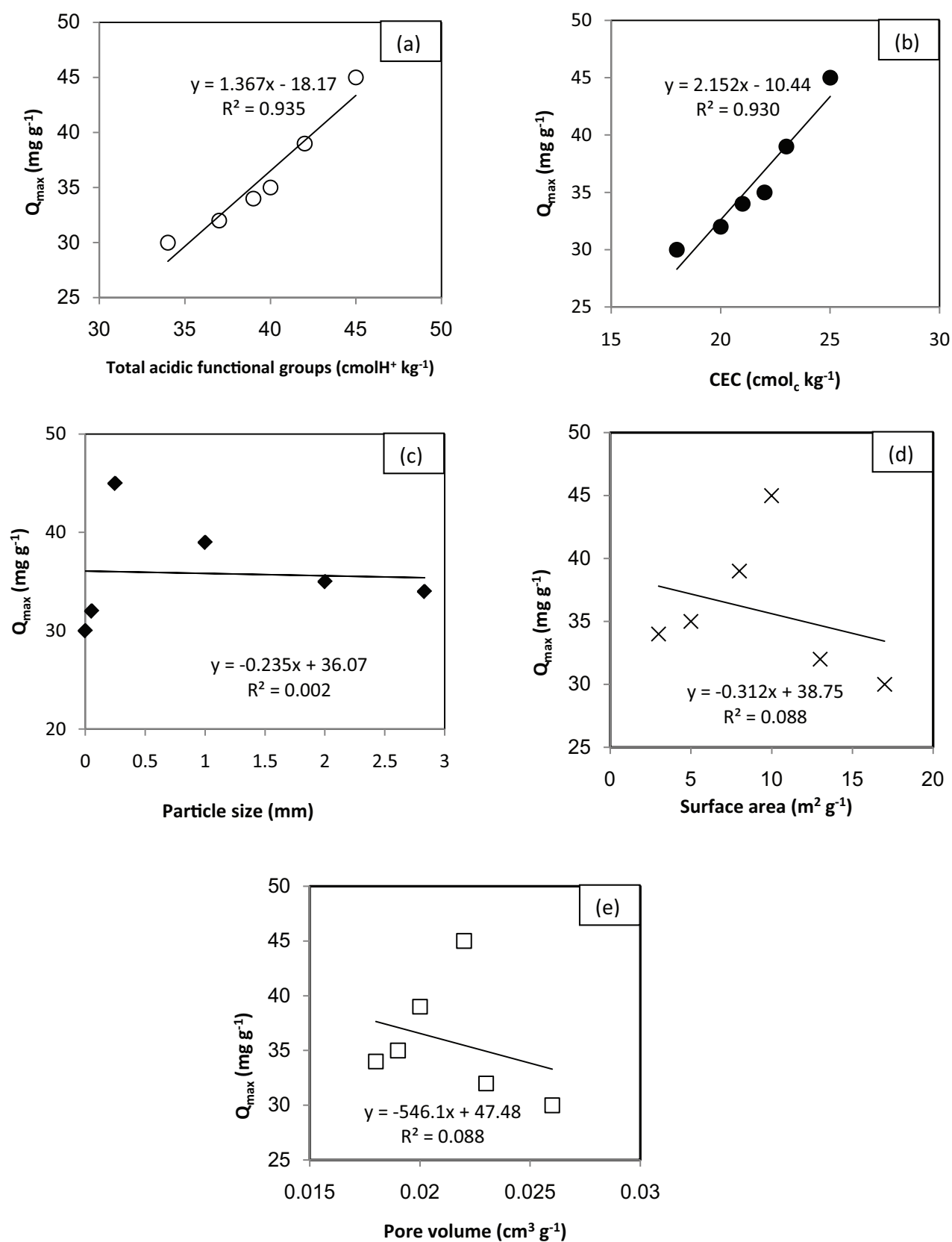
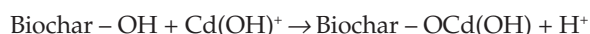
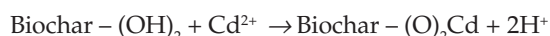
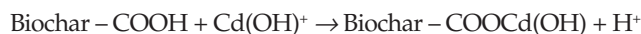
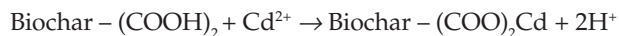


Fig. 5. Correlation between maximum adsorption capacity ( $Q_{max}$ ) of RHB and its characteristics: (a) total acidic functional groups; (b) cation exchange capacity (CEC); (c) particles size; (d) surface area (SA); (e) pore volume (PV).

pH and solution pH had a significant effect on adsorption and precipitation of heavy metals.

The possible adsorption mechanism of Cd on to the some acidic functional groups of biochars can be presented by the following equations:



#### 4. Conclusions

The total acidic functional groups of EFBB was higher than the RHB for similar size class. In contrast, the surface area of RHB was higher than EFBB for similar size class. The  $Q_{max}$  value of EFBB was higher than the value obtained from RHB for similar size class. The EFBB, which had a higher adsorption capacity, was found to be the more effective in removing Cd from aqueous solutions in comparison to a variety of adsorbents. Only total acidic functional groups and CEC were significantly correlated with the  $Q_{max}$  values of both biochars while the PS, SA and PV were not significantly correlated with the  $Q_{max}$ .

#### Acknowledgements

The authors would like to thank Universiti Putra Malaysia for supporting this project under the RUGS grant scheme (Project Number: 01-04-10-0992RU).

#### References

- [1] L. Jarup, Health effects of cadmium exposure—a review of the literature and a risk estimate. *Scand. J. Work Environ. Health*, 24 (1998) 11–51.
- [2] A. Bernard, Cadmium and its adverse effects on human health. *Indian J. Med. Res.*, 128 (2008) 557–564.
- [3] Y.-U. Huange, C.M. Shih, C.J. Huang, C.N. Lin, C.M. Chou, M.L. Tasi, T.P. Liu, C.T. Chen, Effect of cadmium on structure and enzymatic activity of Cu, Zn-SOD and oxidative status in neural cell. *J. Cell. Biochem.*, 98 (2006) 557–589.
- [4] M.M. Rao, D.H. Reddy, P. Venkateswarlu, K. Seshaiyah, Removal of mercury from aqueous using activated carbon prepared from agricultural by-product/waste. *J. Environ. Manage.*, 90 (2009) 634–643.
- [5] L. Beesley, E. Moreno-Jiménez, J.L. Gomez-Eyles, Effects of biochar and green waste compost amendments on mobility, bioavailability and toxicity of inorganic and organic contaminants in a multi-element polluted soil. *Environ. Pollut.*, 158 (2010) 2282–2287.
- [6] M. Uchimiya, I.M. Lima, K.T. Klasson, S.C. Chang, L.H. Wartelle, J.E. Rodger, Immobilization of heavy metal ions (CuII, CdII, NiII, and PbII) by broiler litter-derived biochars in water and soil. *J. Agri. Food Chem.*, 58 (2010) 5538–5544.
- [7] X. Chen, X.G. Chen, L. Chen, Y. Chen, J. Lehmann, M.B. McBride, A.G. Hay, Adsorption of copper and zinc by biochars produced from pyrolysis of hardwood and corn straw in aqueous solution. *Biores. Technol.*, 102 (2011) 8877–8884.
- [8] Z.G. Liu, F.S. Zhang, Removal of lead from water using biochars prepared from hydrothermal liquefaction of biomass. *J. Hazard. Mater.*, 167 (2009) 933–939.
- [9] D. Mohan, Jr C.U. Pittman, M. Bricka, F. Smith, B. Yancey, J. Mohammad, P.H. Steele, M.F. Alexandre-Franco, V.G. Serrano, H. Gong, Sorption of arsenic, cadmium, and lead by chars produced from fast pyrolysis of wood and bark during bio-oil production. *J. Colloid Interf. Sci.*, 310 (2007) 57–73.
- [10] X.S. Wang, L.F. Chen, F.Y. Li, K.L. Chen, Y. Wan, Y.J. Tang, Removal of Cr(VI) with wheat-residue derived black carbon: reaction mechanism and adsorption performance. *J. Hazard. Mater.*, 175 (2010) 816–822.
- [11] S. Yenisoay-Karakas, A. Aygun, M. Gunes, E. Tahtasakal, Physical and chemical characteristics of polymer-based spherical activated carbon and its ability to adsorb organics. *Carbon*, 42 (2004) 477–484.
- [12] Y. Shinogi, Y. Kanri, Pyrolysis of plant, animal and human waste: physical and chemical characterization of the pyrolytic products. *Biores Technol.*, 90 (2003) 241–247.
- [13] S. Fauziah, A. Nurhayati, G. Heiko, S. Adilah, A perspective of oil palm and its wastes. *J. Phys. Sci.*, 21 (2010) 67–77.
- [14] A.W. Samsuri, F. Sadegh-Zadeh, B.J. Seh-Bardan, Adsorption of As(III) and As(V) by Fe coated biochars and biochars produced from empty fruit bunch and rice husk. *J. Environ. Chem. Eng.*, 1 (2013) 981–988.
- [15] A.W. Samsuri, F. Sadegh-Zadeh, B.J. Seh-Bardan, Characterization of biochars produced from oil palm and rice husks and their adsorption capacities for heavy metals. *Inter. J. Environ. Sci. Technol.*, 11 (2014) 967–976.
- [16] D5142., 2009. Standard Test Methods for Proximate Analysis of the Analysis Sample of Coal and Coke by Instrumental Procedures; American Society for Testing and Materials, West Conshohocken, PA.
- [17] H.P. Boehm, Some aspects of the surface chemistry of carbon blacks and other carbons. *Carbon*, 32 (1994) 759–769.
- [18] B.L. Chen, D. Zhou, Z. Lizhong, Transitional adsorption and partition of nonpolar and polar aromatic contaminants by biochars of pine needles with different pyrolytic temperatures. *Environ. Sci. Technol.*, 42 (2008) 5137–5143.
- [19] J. Li, C. Chen, S. Zhang, X. Wang, Surface functional groups and defects on carbon nanotubes affect adsorption-desorption hysteresis of metal cations and oxoanions in water. *Environ. Sci., Nano*, 1 (2014) 488–495.
- [20] Y. Chun, G.Y. Sheng, C.T. Chiou, B.S. Xing, Compositions and sorptive properties of crop residue-derived chars. *Environ. Sci. Technol.*, 38 (2004) 4649–4655.
- [21] S. Shackley, S. Carter, T. Knowles, E. Middelink, S. Haeefe, S. Sohi, A. Cross, S. Haszeldine, Sustainable gasification–biochar systems? A case-study of rice-husk gasification in Cambodia, Part I: Context, chemical properties, environmental and health and safety issues. *Energ. Policy*, 42 (2012) 49–58.
- [22] M. Sciban, M. Kalasnja, B. Skrbic, Modified softwood sawdust as adsorbents for heavy metal ions from water. *J. Hazard. Mater.*, 136 (2006) 266–271.
- [23] B. Benguella, H. Benaissa, Cadmium removal from aqueous solutions by chitin: kinetic and equilibrium studies. *Water Res.*, 36 (2002) 2463–2474.
- [24] C. Moreno-Castilla, M.A. Alvarez-Merino, M.V. Lopez-Ramon, J. Rivera-Utrilla, Cadmium ion adsorption on different carbon adsorbents from aqueous solutions. Effect of surface chemistry, pore texture, ionic strength, and dissolved natural organic matter. *Langmuir*, 20 (2004) 8142–8148.
- [25] Q. Huang, W. Chen, L. Xu, Adsorption of copper and cadmium by Cu and Cd-resistant bacteria and their composites with soil colloids and kaolinite. *Geomicrobiol. J.*, 22 (2005) 227–236.
- [26] P.S. Kumar, K. Ramakrishnan, S.D. Kirupha, S. Sivanesan, Thermodynamic and kinetic studies of cadmium adsorption from aqueous solution onto rice husk. *Braz. J. Chem. Eng.*, 27 (2010) 347–355.
- [27] K.S. Rao, S. Anand, P. Venkateswarlu, Adsorption of Cadmium(II) Ions from Aqueous Solutions by Tectona Grandis L. F. (Teak Leaves Powder). *BioResources*, 5 (2011) 438–454.

- [28] E.I. Unuabonah, K.O. Adebawale, B.I. Olu-Owolabi, L.Z. Yang, L.X. Kong, Adsorption of Pb(II) and Cd (II) from aqueous solutions onto sodium tetraborate-modified Kaolinite clay: equilibrium and thermodynamic studies. *Hydrometallurgy*, 93 (2008) 1–9.
- [29] M. Mohapatra, L. Mohapatra, P. Singh, S. Anand, B.K. Mishra, A comparative study on Pb(II), Cd(II), Cu(II), Co(II) adsorption from single and binary aqueous solutions on additive assisted nano-structured goethite. *Inter. J. Eng. Sci. Technol.*, 2 (2010) 89–103.
- [30] X. Xu, X. Cao, L. Zhao, H. Wang, H. Yu, B. Gao, Removal of Cu, Zn, and Cd from aqueous solutions by the dairy manure-derived biochar. *Environ. Sci. Pollut. Res.*, 20 (2013) 358–368.
- [31] S. Sato, K. Yoshihara, K. Moriyama, M. Machida, H. Tatsumoto, Influence of activated carbon surface acidity on adsorption of heavy metal ions and aromatics from aqueous solution. *Appl. Surf. Sci.*, 253 (2007) 8554–8559.
- [32] K.K. Krishnani, X. Meng, C. Christodoulatos, V.M. Boddu, Biosorption mechanism of nine different heavy metals onto biomatrix from rice husk. *J. Hazard. Mater.*, 153 (2008) 1222–1234.